



Large-scale heavy precipitation over the Czech Republic and its link to atmospheric circulation in CORDEX regional climate models

Romana Beranová¹ · Jan Kyselý^{1,2}

Received: 10 May 2022 / Accepted: 26 February 2024 / Published online: 7 March 2024
© The Author(s) 2024

Abstract

The study evaluates ability of regional climate models (RCMs) to reproduce relationships between large-scale heavy precipitation events (LHPEs) over the Czech Republic and atmospheric circulation. We use an ensemble of 32 RCM simulations with the 0.11° resolution from the Euro-CORDEX project, and compare the historical simulations (1951–2005) against observations from the E-OBS data set. A novel selection criterion for LHPEs is proposed, defining these as days with at least 70% of all grid boxes over a given area with precipitation amounts exceeding the 90th grid-specific percentile of the seasonal distribution of daily amounts. The association with atmospheric circulation is investigated through circulation types derived from sea level pressure using airflow indices (direction, strength and vorticity). The majority of the RCMs capture that the frequency of days with LHPEs is higher in winter than summer, but almost all underestimate the occurrence of LHPEs in both seasons. In winter, the observed LHPEs are connected mainly with cyclonic types and westerly supertype; the role of nonwesterly and cyclonic-nonwesterly superotypes is significant only in the eastern part, where the Atlantic influence is weaker. In summer, the importance of cyclonic and nonwesterly types in producing LHPEs increases compared to winter. The RCMs reasonably well reproduce these links, including differences between seasons and regions, if their ensemble mean is evaluated, but large variations occur among individual simulations mainly in summer. The importance of cyclonic vorticity is overestimated in the RCMs, while westerly advection of moist air plays a smaller role in models than in observations.

Keywords Large-scale heavy precipitation · Atmospheric circulation · Euro-CORDEX RCMs · Central Europe

1 Introduction

River floods are among the most destructive and economically serious weather hazards in Central Europe. During recent decades, several destructive floods hit Central Europe (e.g., the 1997 Oder flood, and the 2002 and 2013 Elbe floods; Müller et al. 2015). The primary cause of large-scale floods within the major river basins in Central Europe is intense, large-scale and long-lasting heavy rain. Due to the profound impacts of floods on human lives, economy, agriculture and infrastructure, there is an urgent need to assess

flood risks in Central Europe. Therefore, it is important to better understand underlying physical mechanisms leading to large-scale heavy precipitation and how they are reproduced in climate models.

Previous studies have analysed large-scale heavy precipitation in Central Europe using several methods. Kašpar and Müller (2008) used daily areal precipitation amounts in predefined sub-regions to identify the most extreme rainfall events; Wypych et al. (2018) evaluated extreme precipitation events related to floods by daily mean areal precipitation totals exceeding 100 mm; and Gvoždíková et al. (2019) selected heavy precipitation by the weather extremity index, reflecting simultaneously the spatial extent and the return periods of daily precipitation totals.

Large-scale heavy precipitation in mid-latitudes is associated mainly with extra-tropical cyclones and atmospheric fronts. A close relationship between atmospheric circulation and heavy precipitation events over Europe has been investigated by a large number of authors (e.g., Bárdossy and

✉ Romana Beranová
rber@ufa.cas.cz

¹ Institute of Atmospheric Physics of the Czech Academy of Sciences, Prague, Czech Republic

² Faculty of Environmental Sciences, Czech University of Life Sciences, Prague, Czech Republic

Filiz 2005; Prudhomme and Geneviev 2011; Irannezhad et al. 2017). An often-discussed issue is the influence of low-pressure systems of Mediterranean origin (cyclones with Vb track) on summer extreme precipitation in Central Europe (Mudelsee et al. 2004; Messmer et al. 2015). Hofstätter et al. (2018) revealed that 45% of all Vb cyclones are connected to heavy precipitation in summer over the Czech Republic and eastern Austria. Niedźwiedź et al. (2015) showed that the occurrence of intense precipitation in the Tatra Mountains (on the Poland/Slovakia border) is strongly related to three circulation types: cyclonic north, cyclonic northeast, and cyclonic trough with varying air flow direction. These situations are associated with cyclones following the Vb track. Large-scale heavy precipitation is also connected to persistence of the governing weather regime (Kurtz et al. 2022).

Regional climate models (RCMs) driven by global climate models (GCMs) are the tools most frequently used for simulating scenarios of climate change at regional and local scales. A number of papers (e.g., Kyselý et al. 2011; Plavcová et al. 2014; Svoboda et al. 2017; Beranová et al. 2018) have analysed RCM simulations of precipitation indices including extremes over Central Europe. Rajczak and Schär (2017) evaluated CORDEX RCMs and found that they perform generally well in the qualitative (i.e., seasonal and geographical variations) and quantitative (i.e., absolute numbers) characterization of the European precipitation climate. They noted that extremes seem to be better captured than is the mean, which obviously suffers from a systematically too high wet-day frequency.

Several studies dealing with validation of control RCM outputs have demonstrated biases in simulating atmospheric circulation in Central Europe. Plavcová and Kyselý (2011) reported too strong advection and overestimation of westerly flow at the expense of easterly flow in most RCMs, which is linked to similar rather general drawbacks in their driving GCMs. The relationships between circulation and precipitation in RCMs have rarely been studied, and this holds true especially when focusing on large-scale heavy precipitation events.

The first goal of this study is to propose a selection criterion for large-scale heavy precipitation events (LHPEs) that considers both precipitation amounts and the extent of the affected area, and at the same time it is easily applicable to model simulations. Then we investigate characteristics of LHPEs over the Czech Republic and their relationships to circulation types, including differences between the western and eastern parts of the examined area that are related to distinct roles of Atlantic and Mediterranean influences on heavy precipitation. The findings are intended to contribute to the understanding of the main driving factors leading to the occurrence of LHPEs in this area. Finally, the ability of CORDEX RCMs to capture the basic circulation-to-precipitation links is examined, which could identify sources of error in the simulated relationships and serve as an important step toward further model improvement. This study represents the initial stage of developing future climate scenarios for the LHPEs using climate model simulations, and better understanding their limitations and uncertainties.

2 Data and methods

2.1 Observed and simulated data

Version 21.0e of the high-resolution European gridded data set (E-OBS; Cornes et al. 2018) is used to represent the observed precipitation. The data set covers the period back to 1950 and provides gridded fields with resolution 0.1° in regular latitude/longitude coordinates. Station density varies significantly over the domain, and also over time. E-OBS works together with 106 stations in the Czech Republic (53 of them with data since 1950, and 93 with data since 1961). Altogether there are 1090 grid boxes over the Czech Republic; for purposes of the study, we have divided the area into the western (557 points, 40 thousand km^2) and the eastern (533 points, 38.5 thousand km^2) parts alongside latitude 15.3°E (Fig. 1). Similar division of the area was used in previous studies on precipitation and its trends (e.g. Kyselý 2009); it is approximately in accordance with main catchments, the Elbe river basin in the western part

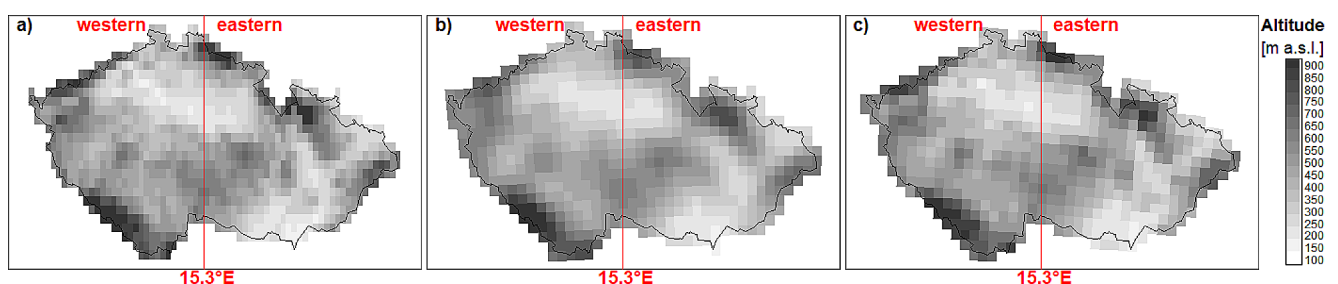


Fig. 1 Orography of the E-OBS data set (a), the CORDEX RCMs (b), and the ALADIN RCM (c). The red line shows how the area of the Czech Republic is divided into the western and the eastern parts

and Oder and Danube river basins in the eastern part, and reflects spatially varied roles of Atlantic and Mediterranean influences on heavy precipitation in Central Europe (Messmer et al. 2015).

Simulated daily precipitation data are taken from the Coordinated Regional climate Downscaling Experiment project (CORDEX; <https://cordex.org/>). We study historical simulations for the European domain (EURO-CORDEX) at the 0.11° resolution (EUR-11; Jacob et al. 2014); those RCMs that had available simulations driven by at least 3 GCMs at the time of the analysis were selected. Seven different RCMs with six driving GCMs are used; together we evaluate 32 RCM simulations (not all RCM-GCM combinations are available) for the 1951–2005 period. The RCMs are listed in Table 1. All RCMs except for ALADIN have the same grid configuration, with 617 grid boxes over the Czech Republic (319 in the western part and 298 in the eastern part). ALADIN has 579 grid boxes (294 in the western part and 285 in the eastern part). Orography and distribution of the grid boxes between the western and the eastern parts of the Czech Republic are shown in Fig. 1. The ability of RCMs to capture the basic features of the European climate, including its variability, was assessed by Kotlarski et al. (2014).

The NCEP/NCAR reanalysis (Kalnay et al. 1996) is used to represent the observed sea level pressure (SLP) data to calculate circulation indices (see Sect. 2.3).

2.2 Criterion for large-scale heavy precipitation event

LHPEs are investigated separately for winter (DJF) and summer (JJA) seasons. Heavy precipitation is defined as daily precipitation amount exceeding the 90th percentile of the distribution of all days in a season over the whole examined period (1951–2005); the thresholds (the 90th percentile) are calculated separately for every grid box, given season, and dataset (E-OBS, RCM simulations).

After several preliminary analyses, LHPEs are then defined as days with at least 70% of all grid boxes over the examined area (the western or the eastern part of the Czech Republic) with heavy precipitation. In some days, such events occur simultaneously in both regions (Fig. 2). Using the threshold of 70% of grid boxes, approximately two-thirds of all days with heavy precipitation (in a given grid box) are related to large-scale events. The result of such a study design is an approximate frequency of occurrence of these events close to 5 days per season, which provides a sufficiently large sample of days for further analysis of the associated circulation types.

Table 1 List of RCMs and their driving GCMs

Institute	RCM	Driving GCMs
Climate Limited-area Modelling Community (CLM)	CCLM	CNRM, HadGEM, ICHEC, MPI
National Centre for Meteorological Research (CNRM)	ALADIN	CNRM, HadGEM, MPI, NCC
Danish Meteorological Institute (DMI)	HIRHAM	CNRM, HadGEM, ICHEC, IPSL, MPI, NCC
Institute for Atmospheric and Climate Science (ETH) in collaboration with the CLM-Community	COSMO	HadGEM, ICHEC, MPI, NCC
Institute Pierre Simon Laplace (IPSL)	WRF	CNRM, HadGEM, ICHEC, IPSL, NCC
Royal Netherlands Meteorological Institute (KNMI)	RACMO	CNRM, HadGEM, ICHEC, IPSL, MPI, NCC
Max Planck Institute for Meteorology (MPI)	REMO	CNRM, IPSL, NCC

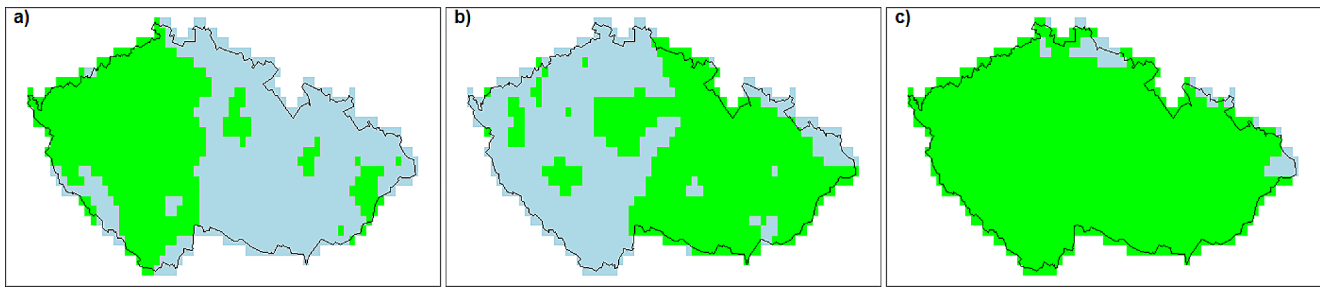


Fig. 2 Example of LHPEs in E-OBS **(a)** in the western part, day 1982-08-06, **(b)** in the eastern part, 1994-07-17, and **(c)** in both parts, 2002-08-11. Grid boxes with precipitation amount exceeding the 90th percentile are coloured green

2.3 Atmospheric circulation

Daily atmospheric circulation characteristics are derived from circulation indices (Jenkinson and Collison 1977). Flow direction, strength and vorticity were calculated from the gridded SLP over Central Europe according to the methodology by Plavcová and Kyselý (2011). Using these indices, we define 27 circulation types: cyclonic (C), anticyclonic (A), 8 straight (directional) types, 16 hybrid types (combination of C and A types with the 8 straight types), and one unclassified (U). Straight types are divided according to flow direction into eight sectors: northeast (NE) 22.5–67.5°, east (E) 67.5–112.5°, southeast (SE) 112.5–157.5° and so forth. The observed circulation types were calculated from the NCEP/NCAR reanalysis SLP data; simulated circulation types were obtained from SLP fields in individual RCMs.

For better visualization and comprehension of relationships between LHPEs and atmospheric circulation, 6 super-types were created (Table 2). The westerly supertype is defined by the predominant flow of moist air masses originating from westerly directions (SW, W, NW), often evolving in the Atlantic Ocean. The cyclonic-westerly supertype blends cyclonic (low-pressure) and westerly atmospheric circulation patterns, typically resulting in unsettled weather and the potential for precipitation. By contrast, the anticyclonic-westerly supertype features high-pressure systems accompanied by westerly flow, frequently leading to stable and fair weather conditions in Central Europe. The nonwesterly supertype encompasses various atmospheric circulation patterns that do not originate from the westward direction, including inflow of dry air from eastern continental Europe, cold and moist air from northern Europe, and warm, moist air from the Mediterranean. The cyclonic-nonwesterly supertype includes circulation types associated with cyclonic systems and air mass flows from directions other than the westerly. Conversely, the anticyclonic-nonwesterly supertype combines anticyclonic conditions with nonwesterly flow. Types C, A and U are not joined into super-types.

3 Results

3.1 Basic precipitation characteristics

Before assessing the ability of RCMs to simulate LHPEs, it is important to evaluate how the RCMs reproduce basic characteristics of precipitation in the examined area. The seasonal precipitation amounts and seasonal 90th percentiles are presented in Fig. 3; the values for the western (eastern) part are displayed by circles (squares), and the colour indicates the driving GCM.

Winter precipitation amounts in E-OBS range between 64 and 333 mm depending on grid box. Mean over the grid boxes is 121 mm and this is almost the same in the western and the eastern parts. Mean over the grid boxes of the winter 90th percentile of daily amounts is 4.2 mm, with a range from 2.3 to 11.8 mm. All RCMs, excluding RACMO_ICHEC and REMO_CNRM, overestimate both seasonal precipitation amounts and the 90th percentile in winter. The overestimation probably relates to the large number of rainy days in RCMs (in some RCMs almost twice as many as in E-OBS, not shown) and enhanced intensity of precipitation (Prein et al. 2016).

In summer, the precipitation amounts and 90th percentiles are higher than in winter in E-OBS, ranging from 178 to 432 mm and from 6 to 14 mm, respectively, depending on grid box. The spatial pattern shows higher values in the eastern than the western part, which is not captured in some RCMs (e.g., CCLM). The difference is larger for the 90th percentile (7.9 mm in the western part while 8.6 mm in the eastern part in E-OBS), and this may be attributed to the more significant role of cyclones of Mediterranean origin in the eastern region. There are significant differences between the individual RCMs; several RCMs substantially underestimate both the precipitation amount and the 90th percentile (e.g., CCLM_HadGEM, COSMO_HadGEM) while WRF overestimates them. Overall, there is no general pattern of the bias for seasonal precipitation amounts, and the 90th percentile tends to be underestimated rather than overestimated by RCMs (Fig. 3).

Table 2 Definition of circulation supertypes and their frequencies in the NCEP/NCAR reanalysis

Supertypes and types C, A, U	Assigned types	
	Frequency [%]	Frequency [%]
	DJF	JJA
westerly (DIR_west)	24.3	14.2
cyclonic-westerly (C_west)	3.6	2.6
anticyclonic-westerly (A_west)	12.1	8.6
nonwesterly (DIR_other)	17.4	18.4
cyclonic-nonwesterly (C_other)	4.1	4.8
anticyclonic-nonwesterly (A_other)	6.7	9.1
cyclonic (C)	6.8	9.3
anticyclonic (A)	24.2	26.0
unclassified (U)	0.8	2.5

3.2 Large-scale heavy precipitation events

The frequency of days with LHPEs is shown in Table 3 and their spatial structure in Fig. 4. The events occurring only in the western (eastern) part are displayed by circles (squares), while events occurring simultaneously in both regions are displayed by triangles.

In E-OBS, the winter frequency of all LHPEs is 6.9% and it is higher than in summer. This is associated with greater importance of frontal stratiform precipitation in the cold part of the year. All RCMs underestimate the frequency of LHPEs, the mean over all RCM simulations being 5.2%. The largest biases are found in HIRHAM simulations (3.6–4.2%, depending on the driving GCM) and for REMO driven by CNRM (4.0%) and IPSL (3.5%). If we look into the spatial structure in observations, there are fewer days with LHPEs occurring only in the eastern part (2.1%) than only in the western (2.4%) or simultaneously in both parts (2.4%). This may be due to a decreasing role of frontal precipitation related to Atlantic influences towards the east. All RCMs capture this pattern and simulate fewer LHPEs in the eastern than western part. The biases in winter are largest for events occurring simultaneously in both regions, the frequency of which is underestimated in all RCMs, most significantly in HIRHAM and REMO. This suggests that the RCMs tend to underestimate the spatial extent of LHPEs in Central Europe.

Summer frequency of all LHPEs is 6.3% in E-OBS (Table 3), and all RCMs except for ALADIN_MPI underestimate it. The lowest values are found in WRF (2.0–2.7%, less than half of the E-OBS values) and REMO (2.6–3.4%). All HIRHAM and some ALADIN simulations (driven by HadGEM and MPI) provide higher percentage of days with LHPEs in summer than in winter. Overall, this pattern, which contradicts observations, is found in 9 out of the 32 RCM simulations.

The spatial distribution of summer LHPEs in observations is as follows (Fig. 4): 2.7% in the western part, 2.4% in the eastern part, and 1.2% simultaneously in both regions. The LHPEs occurring in both areas simultaneously are related to larger-scale synoptic patterns (typically cyclones and frontal passages), and that is why they are much less frequent in JJA (when convective processes are important) than events occurring in a single region only. All RCMs capture the relatively small percentage of events affecting the whole area simultaneously. However, some RCM simulations lead to more events in the eastern than in the western part (e.g., ALADIN, HIRHAM_HadGEM, HIRHAM_IPSL, WRF_IPSL, RACMO_NCC).

Fig. 3 Mean over the grid boxes of seasonal precipitation amounts (upper graphs) and 90th percentiles of daily precipitation (Q90, lower graphs) in winter (left) and summer (right)

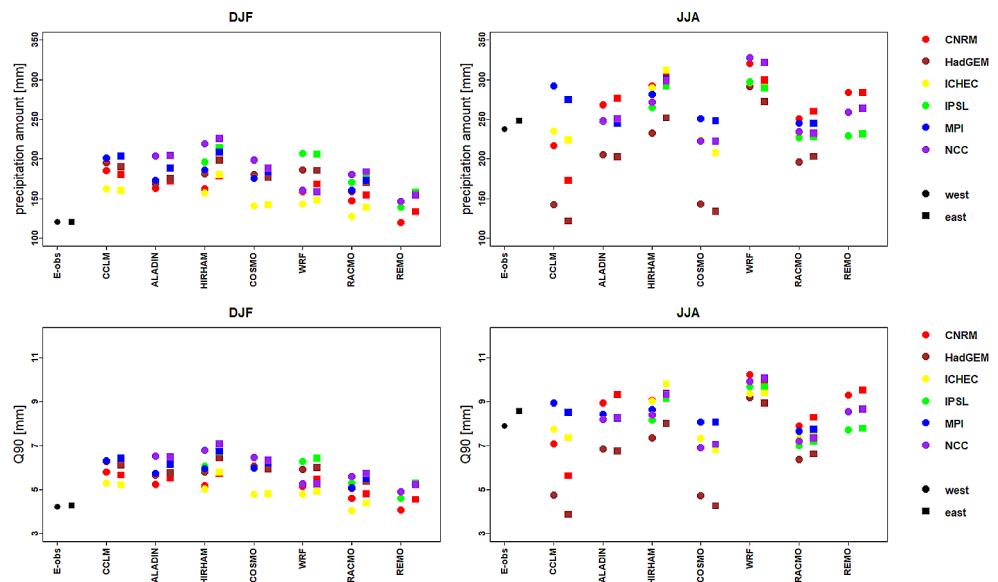


Table 3 Seasonal frequency of days with LHPEs

	Frequency [%]		Frequency [%]		
	DJF	JJA	DJF	JJA	
E-OBS	6.9	6.3	RCM mean	5.2	4.7
CCLM_CNRM	6.4	4.4	WRF_CNRM	5.4	2.2
CCLM_HadGEM	6.5	5.9	WRF_HadGEM	4.8	2.3
CCLM_ICHEC	6.2	5.4	WRF_ICHEC	5.3	2.7
CCLM_MPI	6.2	5.3	WRF_IPSL	4.9	2.0
ALADIN_CNRM	5.7	5.7	WRF_NCC	6.0	2.4
ALADIN_HadGEM	5.5	5.8	RACMO_CNRM	5.7	5.3
ALADIN_MPI	5.8	6.4	RACMO_HadGEM	5.8	5.5
ALADIN_NCC	5.9	5.7	RACMO_ICHEC	5.6	6.0
HIRHAM_CNRM	4.1	5.2	RACMO_IPSL	5.6	5.5
HIRHAM_HadGEM	3.9	5.1	RACMO_MPI	5.9	5.9
HIRHAM_ICHEC	4.2	5.5	RACMO_NCC	5.7	5.4
HIRHAM_IPSL	3.6	5.0	REMO_CNRM	4.0	2.6
HIRHAM_MPI	4.2	5.0	REMO_IPSL	3.5	3.4
HIRHAM_NCC	4.1	4.6	REMO_NCC	5.0	2.8
COSMO_HadGEM	5.8	5.7	COSMO_MPI	6.5	5.4
COSMO_ICHEC	5.7	5.3	COSMO_NCC	5.9	4.6

3.3 Atmospheric circulation types

Boxplots of the frequencies of circulation types are shown in Fig. 5. In the NCEP/NCAR reanalysis the most frequent winter circulation types or supertypes (cf. Section 2.3 and Table 2) are westerly (DIR_{west}, 24%), anticyclonic (A, 24%), nonwesterly (DIR_{other}, 17%), and anticyclonic-westerly (A_{west}, 12%). All RCMs overestimate the frequency of the westerly supertype. In RCM simulations driven by IPSL and NCC, the westerly supertype occurs on 35–40% of all days. On the other hand, the frequency of nonwesterly supertype is underestimated by all RCMs, with the

largest underestimation found again in those RCMs driven by IPSL and NCC. Deficiencies, although with different magnitudes or sometimes even with different signs, were found also in frequencies of anticyclonic (A) and cyclonic (C) types. Some models underestimate the frequency of the anticyclonic type (e.g., WRF_IPSL, frequency 10%) and at the same time overestimate that of the cyclonic type (WRF_IPSL, 15.5%, which is more than twice compared to the reanalysis).

The most frequent summer circulation types and super-types in the NCEP/NCAR reanalysis are anticyclonic (26%), nonwesterly (18%) and westerly (14%). The RCMs simulate summer circulation types fairly well, with less pronounced biases compared to winter. There is no circulation type that would be overestimated or underestimated by all RCMs. Some RCMs, mainly driven by MPI and NCC, overestimate the frequency of anticyclonic type while others, mainly driven by CNRM, underestimate it. Individual RCMs also overestimate frequencies of nonwesterly supertype (e.g., WRF_CNRM 28%, WRF_IPSL 33%). Several RCMs driven by MPI strongly overestimate the frequency of westerly supertype (CCLM_MPI 21%, HIRHAM_MPI 20%) while RCMs driven by HadGEM strongly underestimate it (COSMO_HadGEM and CCLM_HadGEM 5%).

3.4 Links between large-scale heavy precipitation and circulation

Frequencies of all circulation supertypes during winter LHPEs in the western and the eastern parts and simultaneously occurring in both regions are shown in Fig. 6. The first column stands for E-OBS, while the second shows ensemble means of all RCM simulations, and individual RCMs follow. In observations, winter LHPEs are connected mainly

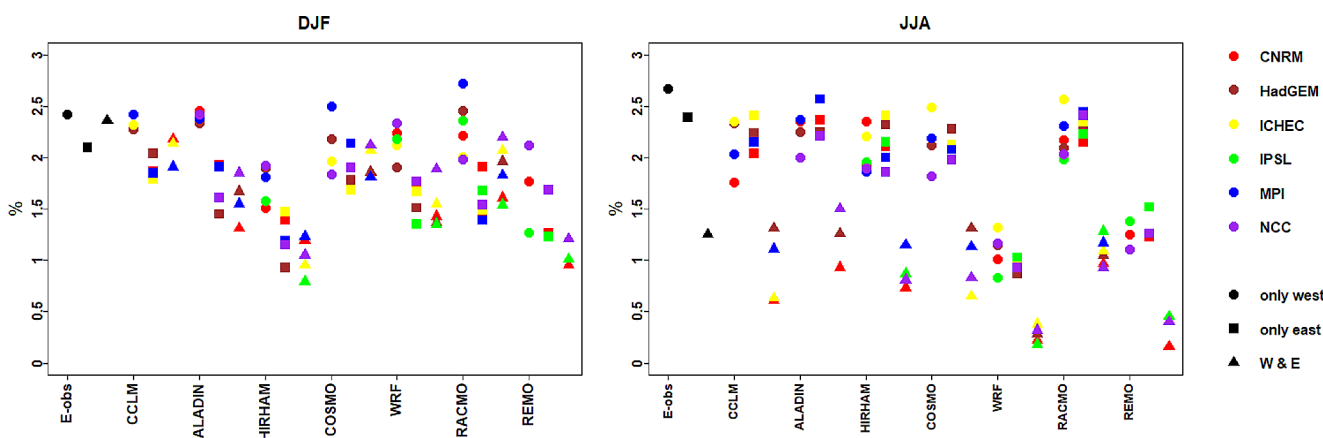
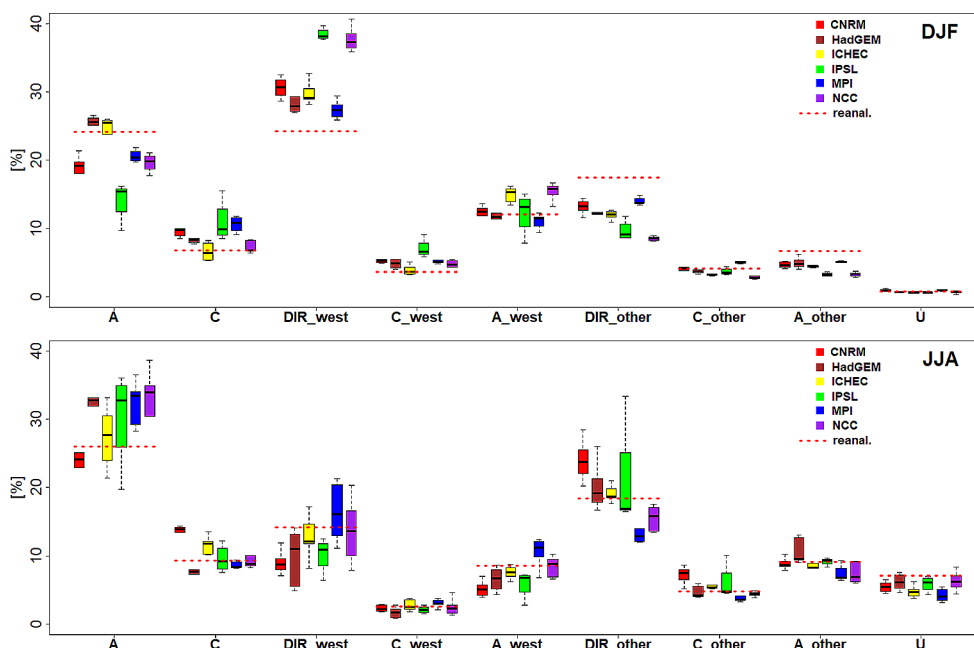


Fig. 4 Frequency of days with LHPEs. Events occurring only in the western (eastern) part are displayed by circles (squares), while events occurring simultaneously in both regions are displayed by triangles

Fig. 5 Boxplots of the frequency of circulation types and super-types in winter (upper graph) and summer (lower graph). The boxplots are calculated across individual RCMs driven by the same GCMs. The driving GCMs are indicated by colours. The red dotted lines display the frequency of circulation types and super-types in the NCEP/NCAR reanalysis

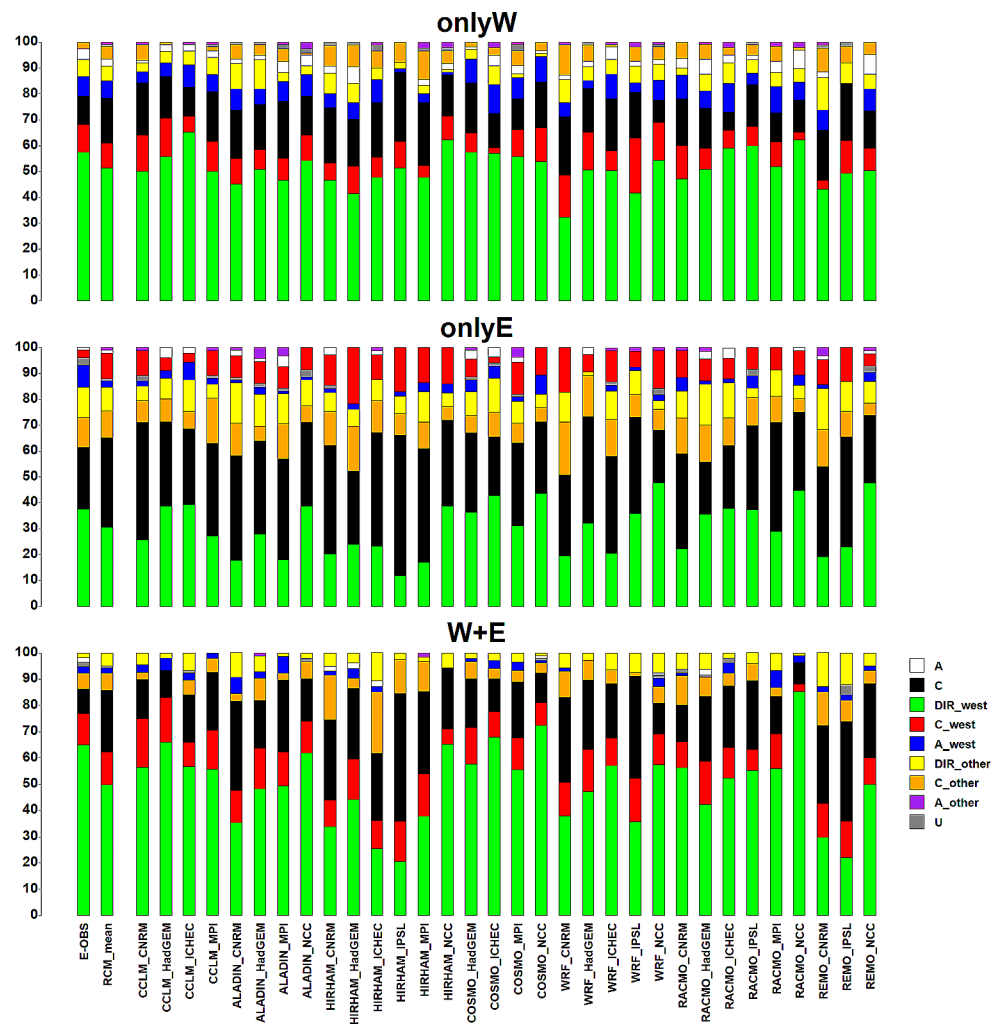


with westerly, cyclonic-westerly and cyclonic supertypes, frequencies of which are more than doubled compared to mean winter occurrence (cf. Table 2; Fig. 6).

There are significant differences in the link of LHPEs to circulation between the western and the eastern parts in winter (Fig. 6). In observations, the events in the western part are mainly connected with westerly supertype (58%), cyclonic type (11%), and cyclonic-westerly supertype (11%), with nonwesterly supertype occurring infrequently during LHPEs (7%). Events in the eastern part are also linked to westerly supertype, but only in 38%, followed by cyclonic type (24%); nonwesterly and cyclonic-nonwesterly supertypes are more frequent (together 23%) than in the western part. Events occurring simultaneously in both parts are linked mainly to westerly supertype (65%).

The majority of RCMs reasonably well simulate differences in circulation-to-precipitation link between the western and the eastern parts during winter. Nearly all RCMs (except for WRF_NCC and RACMO_HadGEM) overestimate frequency of the cyclonic type during LHPEs in both parts. This overestimation is larger in the eastern part mainly in HIRHAM simulations (e.g., HIRHAM_IPSL 54%), CCLM_CNRM (45%) and RACMO_MPI (42%). In the western part, some RCMs underestimate the frequency of westerly supertype (e.g., HIRHAM_HadGEM at 41%, WRF_CNRM at 32%), most RCMs driven by CNRM overestimate the role of nonwesterly supertype (ALADIN_CNRM 10%, REMO_CNRM 12.5%), and several RCMs overestimate the role of cyclonic-nonwesterly supertype (WRF_CNRM 12%, HIRHAM_MPI 11%). Many RCMs underestimate frequency of westerly supertype and

Fig. 6 Frequency of circulation types and supertypes connected with winter LHPEs. Top: LHPEs only in the western part, middle: LHPEs only in the eastern part, bottom: LHPEs simultaneously in both regions. In all columns, the types are ordered according to their frequency in E-OBS

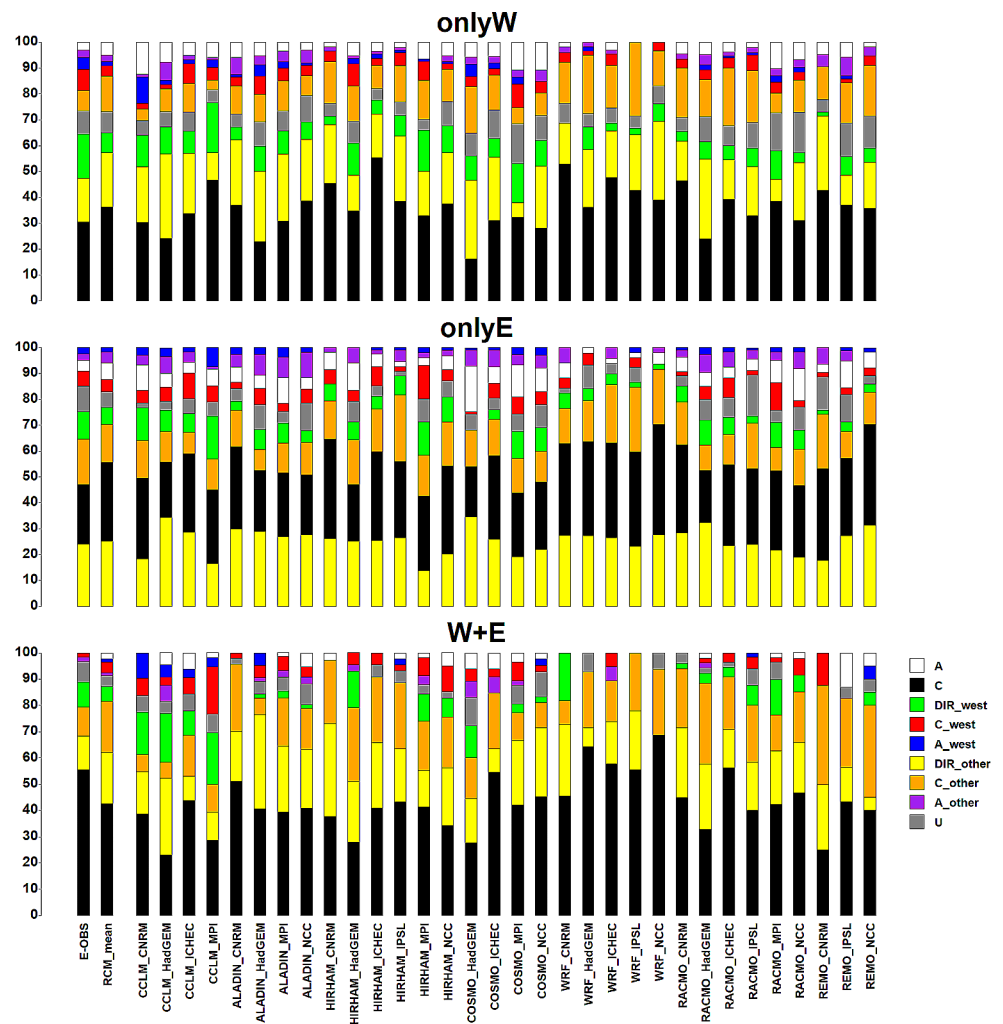


overestimate frequency of cyclonic type during events simultaneously occurring in both parts (HIRHAM_ICHEC, REMO_IPSL).

Connections between summer LHPEs occurring in the western, eastern and both parts and circulation types are shown in Fig. 7. The differences between the western and the eastern parts are not so large in comparison to winter. In observations, LHPEs in the western part are linked mainly to cyclonic type (30%), while westerly and nonwesterly supertypes are represented with the same frequency (17%). Occurrence of cyclonic type during LHPEs is more than three times higher than mean summer frequency (Table 2). Precipitation events in the eastern part are connected mainly with nonwesterly (24%) and cyclonic-nonwesterly supertypes (17%, more than three times higher than mean summer frequency). The frequencies of cyclonic type (23%) and westerly supertype (11%) are smaller compared to those during events occurring in the western part. The prevailing type during LHPEs simultaneously occurring in both parts is the cyclonic type with frequency 56%, which is 6 times higher than summer climatology.

There are considerable differences between individual RCMs in simulation of circulation-to-precipitation links in summer. Some RCMs strongly overestimate the role of cyclonic circulation mainly in the western part: all WRF simulations (e.g., WRF_ICHEC 48%), as well as CCLM_MPI (47%) and HIRHAM_ICHEC (55%). Some RCMs underestimate the occurrence of westerly supertype during LHPEs; this concerns the majority of those RCMs driven by CNRM, as well as REMO and WRF RCMs. Some models connect LHPEs with anticyclonic type (CCLM_CNRM, COSMO_MPI, REMO_IPSL). Only a few simulations capture similarly strong links between events simultaneously occurring in both parts and the cyclonic type as found in E-OBS: ALADIN_CNRM (frequency of C type during LHPEs is 51%), COSMO_ICHEC (55%), WRF_ICHEC (58%), and RACMO_ICHEC (56%). Overall, these results are influenced by relatively small frequencies of LHPEs, especially those occurring simultaneously in the whole area, in some RCMs.

Fig. 7 As in Fig. 6, except for summer



4 Discussion

The threshold for heavy precipitation can be set by a number of different methodologies. The simplest method is to use a fixed threshold, such as 10 mm per day (Zhang et al. 2011), which does not reflect local characteristics of the precipitation. Another method is to use a wet-day percentile (e.g., 75th) as a threshold. In this case precipitation percentiles are computed for the subset of days with non-zero precipitation. This method is appropriate only for observational data, however. If comparison of observations and RCM simulations is the goal, then this method is unsuitable because of the generally overestimated numbers of rainy days in RCMs (Rajczak and Schär 2017). Heavy precipitation thresholds defined in this way are underestimated by RCMs and numbers of days with heavy precipitation are overestimated. That is why we defined the threshold for heavy precipitation as all-day percentile (90th), in line with the recommendation by Ban et al. (2015), for example.

We have proposed a selection criterion for large-scale heavy precipitation that should be able to identify

precipitation events potentially leading to large-scale floods. Heavy rainfall during 11–13 August 2002 that, together with previous catchment saturation (Schröter et al. 2015), caused destructive Elbe/Vltava floods (Ulbrich et al. 2003) is an example. Our method captured this situation very well: on 11 August large-scale heavy precipitation simultaneously occurred in both parts of the area (Fig. 2, right map), LHPE is identified on 12 August in the western part and on 13 August in the eastern part. Our method captures also the preceding LHPEs on 4, 6 and 7 August 2002 that contributed to saturation of catchments before the main flood event.

Driving circulation types of LHPEs differ between winter and summer. In winter, LHPEs are primarily associated with westerly supertype, cyclonic-westerly supertype, and cyclonic type. These circulation patterns bring moist air masses originating in the Atlantic Ocean and are often associated with cyclones and frontal passages. Nonwesterly supertypes play a significant role primarily in the eastern part, where the influence of the Mediterranean Sea is prominent. In contrast, during summer, the dominant circulation type is cyclonic. Both westerly supertype and nonwesterly

supertypes play similar roles, and the differences between the western and eastern parts are not as pronounced. This can be explained by a smaller role of frontal systems from the west and prevailing convective processes in summer.

The ability of RCMs to simulate precipitation characteristics and circulation types depends on season. In winter, almost all RCMs have a tendency to overestimate the 90th percentile of daily amounts (Q90), underestimate the total number of LHPEs, overestimate frequency of the westerly supertype, and underestimate frequency of the nonwesterly supertype. In summer, the general tendencies of biases are less pronounced and differences between individual RCMs are larger (Figs. 3, 4 and 5); some models show a strong relationship between Q90 value and the frequency of westerly supertype (e.g., COSMO_HadGEM, CCLM_HadGEM). These differences are given mainly by different parameterization schemes of convection in RCMs. Our results are in qualitative terms in agreement with Vautard et al. (2021), who showed that the inter-model spread is larger in summer than in winter.

Substantial drawbacks in winter are found for events occurring simultaneously in both parts of the examined area. These LHPEs are strongly underestimated by RCMs, and, while in the observed data they occur under westerly circulation (westerly, cyclonic-westerly and anticyclonic-westerly supertypes) in nearly 80% of days, this percentage is below 40% in some RCMs (HIRHAM_ICHEC, HIRHAM_IPSL, REMO_IPSL), and nearly all models generally overestimate the role of cyclonic type in these events. This suggests that the importance of cyclonic vorticity in producing LHPEs in Central Europe is overestimated in RCMs, while westerly advection of moist air plays a smaller role in models than in observations.

5 Conclusions

We have proposed a novel selection criterion for large-scale heavy precipitation events (LHPEs), defining these as days with at least 70% of all grid boxes over the examined area with heavy precipitation (exceeding the grid-specific 90th percentile of the distribution of all days in a given season). We analysed relationships between these events and circulation during 1951–2005 in observations (E-OBS gridded data set for precipitation, NCEP/NCAR reanalysis for SLP from which circulation types were derived), and an ensemble of 32 Euro-CORDEX RCM simulations with the 0.11° resolution was evaluated to assess ability to reproduce the circulation-to-precipitation links.

The main findings of the present study can be summarized as follows:

- In observations, the frequency of all LHPEs in winter (6.9%) is slightly higher than in summer (6.3%). In winter, the numbers of events occurring in the western, in the eastern and simultaneously in both parts of the studied area are approximately equal while in summer, LHPEs occurring simultaneously in both parts are in a minority.
- Almost all RCMs underestimate frequency of LHPEs in both winter and summer. The RCMs tend to underestimate the spatial extent of LHPEs in Central Europe.
- In winter, the observed LHPEs are connected mainly with cyclonic type and westerly supertype. The link to nonwesterly and cyclonic-nonwesterly supertypes is important only in the eastern part. The majority of RCMs capture differences in circulation-to-precipitation links between the western and the eastern parts but almost all RCMs overestimate the frequency of cyclonic type during LHPEs.
- In summer, the observed LHPEs are associated mainly with cyclonic type, as well as westerly and nonwesterly supertypes. The differences between the western and the eastern parts are not so large in comparison with winter. The prevailing type during events simultaneously occurring in both parts is cyclonic type with frequency 56%, which is 6 times higher than is its mean summer occurrence.
- There are considerable differences between individual RCMs in simulation of circulation-to-precipitation links in summer. Only a few models are able to simulate the strong link between events simultaneously occurring in both parts and cyclonic type, which is related to underestimated spatial extent of LHPEs in summer.
- The results suggest that in generating LHPEs, the importance of cyclonic vorticity is overestimated in RCMs while westerly advection of moist air from the Atlantic plays a smaller role than in observations.

In conclusion, the method proposed for LHPEs is able to capture the precipitation events potentially leading to floods, and it may be suitable to characterize also the flood-risk conditions in future climate scenarios.

Acknowledgements We acknowledge the E-OBS dataset from the EU-FP6 project UERRA (<http://www.uerra.eu>) and the data providers in the ECA&D project (<https://www.ecad.eu>). The authors acknowledge the CORDEX initiative, especially the EURO-CORDEX project, for providing RCM data. The study was supported by the Czech Science Foundation (project no. 20-28560 S).

Author contributions Both authors contributed to the study conception, design and interpretation of the results. R.B. prepared and analyzed data and wrote the first draft of the manuscript. Both authors read and approved the final manuscript.

Funding This work was supported by the Czech Science Foundation (project no. 20-28560 S).

Open access publishing supported by the National Technical Library in Prague.

Data availability The E-OBS dataset comes from the EU-FP6 project UERRA (<http://www.uerra.eu>), and the data are provided by the ECA&D project (<https://www.ecad.eu>). The NCEP/NCAR reanalysis is available from <https://psl.noaa.gov/data/gridded/data.ncep.reanalysis.html>. The RCM data used and analysed during current study comes from the EURO-CORDEX project and are available in <https://cordex.org/>.

Code Availability Not applicable.

Declarations

Conflict of interest The authors have no competing interests to declare that are relevant to the content of this article.

Ethics approval Not applicable.

Consent to participate Both authors made substantial contributions to the conception or design of the work.

Consent for publication Both authors agree with publication.

Open Access This article is licensed under a Creative Commons Attribution 4.0 International License, which permits use, sharing, adaptation, distribution and reproduction in any medium or format, as long as you give appropriate credit to the original author(s) and the source, provide a link to the Creative Commons licence, and indicate if changes were made. The images or other third party material in this article are included in the article's Creative Commons licence, unless indicated otherwise in a credit line to the material. If material is not included in the article's Creative Commons licence and your intended use is not permitted by statutory regulation or exceeds the permitted use, you will need to obtain permission directly from the copyright holder. To view a copy of this licence, visit <http://creativecommons.org/licenses/by/4.0/>.

References

- Ban N, Schmidli J, Schär C (2015) Heavy precipitation in a changing climate: does short-term summer precipitation increase faster? *Geophys Res Lett* 42:1165–1172. <https://doi.org/10.1002/2014GL062588>
- Bárdossy A, Filiz F (2005) Identification of flood producing atmospheric circulation patterns. *J Hydrol* 313:48–57. <https://doi.org/10.1016/j.jhydrol.2005.02.006>
- Beranová R, Kyselý J, Hanel M (2018) Characteristics of sub-daily precipitation extremes in observed data and regional climate model simulations. *Theor Appl Climatol* 132:515–527. <https://doi.org/10.1007/s00704-017-2102-0>
- Cornes RC, van der Schrier G, van den Besselaar EJM, Jones PD (2018) An Ensemble Version of the E-OBS temperature and precipitation datasets. *J Geophys Res Atmos* 123:9391–9409. <https://doi.org/10.1029/2017JD028200>
- Gvoždíková B, Müller M, Kašpar M (2019) Spatial patterns and time distribution of central European extreme precipitation events between 1961 and 2013. *Int J Climatol* 39:3282–3297. <https://doi.org/10.1002/joc.6019>
- Hofstätter M, Lexer A, Homann M, Blöschl G (2018) Large-scale heavy precipitation over central Europe and the role of atmospheric cyclone track types. *Int J Climatol* 38:e497–e517. <https://doi.org/10.1002/joc.5386>
- Irannezhad M, Chen D, Kløve B, Moradkhani H (2017) Analysing the variability and trends of precipitation extremes in Finland and their connection to atmospheric circulation patterns. *Int J Climatol* 37:1053–1066. <https://doi.org/10.1002/joc.5059>
- Jacob D, Petersen J, Eggert B et al (2014) EURO-CORDEX: new high-resolution climate change projections for European impact research. *Reg Environ Change* 14:563–578. <https://doi.org/10.1007/s10113-013-0499-2>
- Jenkinson AF, Collison FP (1977) An initial climatology of gales over the North Sea. Synoptic Climatology Branch Memorandum No 62, Meteorological Office, Bracknell, UK
- Kalnay E, Kanamitsu M, Kistler R et al (1996) The NCEP/NCAR 40-Year Reanalysis Project. *B Am Meteorol Soc* 77:437–471
- Kašpar M, Müller M (2008) Selection of historic heavy large-scale rainfall events in the Czech Republic. *Nat Hazards Earth Syst Sci* 8:1359–1367. <https://doi.org/10.5194/nhess-8-1359-2008>
- Kautz L-A, Martius O, Pfahl S, Pinto JG, Ramos AM, Sousa PM, Woollings T (2022) Atmospheric blocking and weather extremes over the Euro-Atlantic sector – a review. *Weather Clim Dynam* 3:305–336. <https://doi.org/10.5194/wcd-3-305-2022>
- Kotlarski S, Keuler K, Christensen OB et al (2014) Regional climate modeling on European scales: a joint standard evaluation of the EURO-CORDEX RCM ensemble. *Geosci Model Dev* 7:1297–1333. <https://doi.org/10.5194/gmd-7-1297-2014>
- Kyselý J (2009) Trends in heavy precipitation in the Czech Republic over 1961–2005. *Int J Climatol* 29:1745–1758. <https://doi.org/10.1002/joc.1784>
- Kyselý J, Gaál L, Beranová R, Plavcová E (2011) Climate change scenarios of precipitation extremes in Central Europe from ENSEMBLES regional climate models. *Theor Appl Climatol* 104:529–542. <https://doi.org/10.1007/s00704-010-0362-z>
- Messmer M, Gómez-Navarro JJ, Raible CC (2015) Climatology of Vb cyclones, physical mechanisms and their impact on extreme precipitation over Central Europe. *Earth Syst Dynam* 6:541–553. <https://doi.org/10.5194/esd-6-541-2015>
- Mudelsee M, Börngen M, Tetzlaff G, Grünwald U (2004) Extreme floods in central Europe over the past 500 years: role of cyclone pathway Zugstrasse Vb. *J Geophys Res Atmos* 109:D23101. <https://doi.org/10.1029/2004JD005034>
- Müller M, Kašpar M, Valeriánová A, Crhová L, Holtanová E, Gvoždíková B (2015) Novel indices for the comparison of precipitation extremes and floods: an example from the Czech territory. *Hydrol Earth Syst Sci* 19:4641–4652. <https://doi.org/10.5194/hess-19-4641-2015>
- Niedźwiedz T, Łupikasza E, Pińskwar I, Kundzewicz ZW, Stoffel M, Małarzewski Ł (2015) Variability of high rainfalls and related synoptic situations causing heavy floods at the northern foothills of the Tatra Mountains. *Theor Appl Climatol* 119:273–284. <https://doi.org/10.1007/s00704-014-1108-0>
- Plavcová E, Kyselý J (2011) Evaluation of daily temperatures in Central Europe and their links to large-scale circulation in an ensemble of regional climate models. *Tellus* 63:763–781. <https://doi.org/10.1111/j.1600-0870.2011.00514.x>
- Plavcová E, Kyselý J, Štěpánek P (2014) Links between circulation types and precipitation in Central Europe in the observed data and regional climate model simulations. *Int J Climatol* 34:2885–2898. <https://doi.org/10.1002/joc.3882>
- Prein AF, Gobiet A, Truhetz H et al (2016) Precipitation in the EURO-CORDEX 0.11° and 0.44° simulations: high resolution, high. Benefits? *Clim Dynam* 46:383–412. <https://doi.org/10.1007/s00382-015-2589-y>

- Prudhomme C, Geneviev M (2011) Can atmospheric circulation be linked to flooding in Europe? *Hydrol Process* 25:1180–1190. <https://doi.org/10.1002/hyp.7879>
- Rajczak J, Schär C (2017) Projections of future precipitation extremes over Europe: a Multimodel Assessment of Climate simulations. *J Geophys Res Atmos* 122 10,773–10,800. <https://doi.org/10.1002/2017JD027176>
- Schröter K, Kunz M, Elmer F, Mühr B, Merz B (2015) What made the June 2013 flood in Germany an exceptional event? A hydro-meteorological evaluation. *Hydrol Earth Syst Sci* 19:309–327. <https://doi.org/10.5194/hess-19-309-2015>
- Svoboda V, Hanel M, Máca P, Kyselý J (2017) Characteristics of rainfall events in RCM simulations for the Czech Republic. *Hydrol Earth Syst Sci* 21:963–980. <https://doi.org/10.5194/hess-2016-283>
- Ulbrich U, Brücher T, Fink AH, Leckebusch GC, Krüger A, Pinto JG (2003) The central European floods of August 2002. Part I: rainfall periods and flood development. *Weather* 58:371–377. <https://doi.org/10.1256/wea.61.03A>
- Vautard R, Kadyrov N, Iles C et al (2021) Evaluation of the large EURO-CORDEX Regional Climate Model Ensemble. *J Geophys Res Atmos* 126. <https://doi.org/10.1029/2019JD032344>
- Wypych A, Ustrnul Z, Czekierda D, Palarz A, Sulikowska A (2018) Extreme precipitation events in the Polish carpathians and their synoptic determinants. *Időjárás* 122:145–158. <https://doi.org/10.28974/idojaras.2018.2.3>
- Zhang X, Alexander L, Hegerl GC, Jones P, Tank AK, Peterson TC, Trewin B, Zwiers FW (2011) Indices for monitoring changes in extremes based on daily temperature and precipitation data. *WIREs: Clim Change* 2:851–870. <https://doi.org/10.1002/wcc.147>

Publisher's Note Springer Nature remains neutral with regard to jurisdictional claims in published maps and institutional affiliations.